Two-Phase MMC Based on Modular Multilevel Series/Parallel Converter for Back to Back Power Systems

Fierro, Felipe ; Lizana F., Ricardo; Alcaide, Abraham M.; Rivera, Sebastian

DOI
10.1109/CHILECON60335.2023.10418757

Publication date
2023

Document Version
Final published version

Published in
Proceedings of the 2023 IEEE CHILEAN Conference on Electrical, Electronics Engineering, Information and Communication Technologies (CHILECON)

2023 IEEE CHILEAN Conference on Electrical, Electronics Engineering, Information and Communication Technologies (CHILECON) | 979-8-3503-6953-3/23/$31.00 ©2023 IEEE | DOI: 10.1109/CHILECON60335.2023.10418757

Two-Phase MMC based on Modular Multilevel Series/Parallel Converter for back to back power systems

1st Felipe Fierro
Centro de Energia
UCSC
Concepcion, Chile
ffierro@magister.ucsc.cl

2nd Ricardo Lizana F.
Centro de Energia
UCSC
Concepcion, Chile
ricardolizana@ucsc.cl

3rd Abraham M. Alcaide
Electronic Department
Universidad de Sevilla
41092 Sevilla, Spain
amarquez@ieee.org

4th Sebastian Rivera
Electrical Sustainable Energy - DCE&S
Delft University of Technology
Delft 2628 CD, Netherlands
s.rivera.i@ieee.org

***Abstract*—The MMC converter is the key topology for HVDC applications. In these systems, a major complexity is the number of modules and components required per phase to achieve nominal voltage and current levels for applications in transmission system. In this paper, the topology and control of a two-phase MMC system for HVDC applications is presented. The main idea is to eliminate a complete phase of the classic MMC converter for reduce the number of modules and the complexity of the system, together with the use of MMSPC-type modules, in order to achieve internal voltage balance without the need of extra sensors and control loops.**

I. Introduction

MODULAR multilevel converters (MMC) have evolved into the perfect option for HVDC transmission systems. This is because the MMC offers multiples advantages compared with other traditional VSC power topologies, such as reduced current/voltage total harmonic distortion (THD) performance, reduced commo-mode voltage, modularity, scalability and decoupled control of active and reactive power, to name a few [1]–[5]. On the other hand, the MMC needs to control different variables for achieve a correct operation, like the voltage balance among the modules, DC-link current, AC side currents and circulating currents [6].

To achieve the control of some of these variables in an inherent way, the key is the selection of the type of module that acts as the building block for the MMC. Among the recently proposed topologies, the Modular Multilevel Series Parallel Converter (MMSPC) offers the ability to connect not only the modules in series or bypass, but also allows the modules to be connected in parallel, allowing the internal voltage balance of the modules without sensor requirements or complex control loops [7]–[10].

However, regardless of the type of module that is selected to be used, one of the biggest considerations when using a MMC is the large number of modules that are required per phase, in order to achieve the required voltage/current levels. In commercial MMC prototypes, the number of modules per arm reaches $N = 216$, which implies a significant challenge in terms of control and communication platforms, together with the implementation of these systems [2].

979-8-3503-6953-3/23/$31.00 2023 IEEE

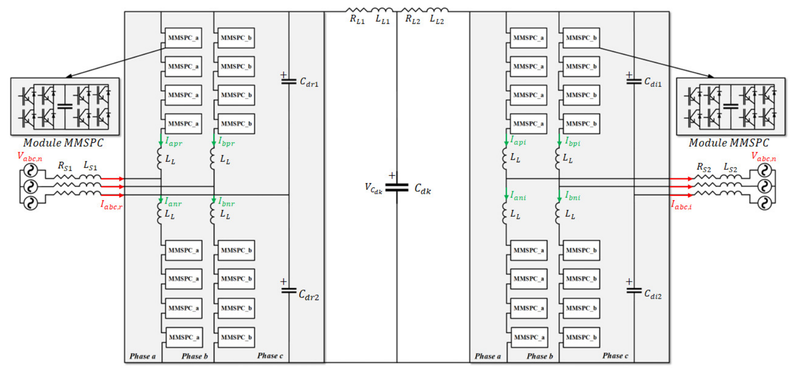

Figure 1: Proposed system

In this work, a system based on two MMCs connected back to back, each composed of only two phases, is presented. The proposed system allows to control the 3-phase currents of both AC systems, together with maintaining the internal balance of the modules thanks to the fact that they are based on MMSPC configuration. The objective of this work is to significantly reduce the number of semiconductors and complexity of the system, given the elimination of a complete phase each of the MMCs.

II. Topology description

The proposed system configuration is illustrated in Fig. 1, which is obtained by coupling a two-phase rectifier and two-phase inverter (Fig. 2 and Fig. 3 respectively). Each phase of the converter is composed by two arms, the positive and negative arm, and each arm of the proposed system is composed of several (N) modules based on a modular multilevel series/parallel converter (MMSPC). The reason behind the use of MMSPC modules is to enable a simpler balancing strategy among the modules [9], [11]–[13].

The aforementioned structure resembles the traditional MMC, given that the DC system is connected at the extremes

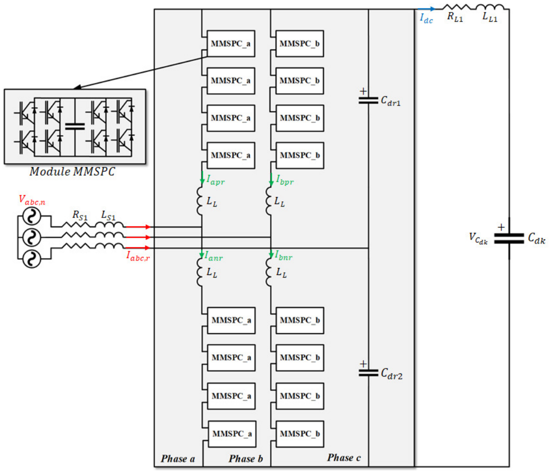

Figure 2: Two phase rectifier topology

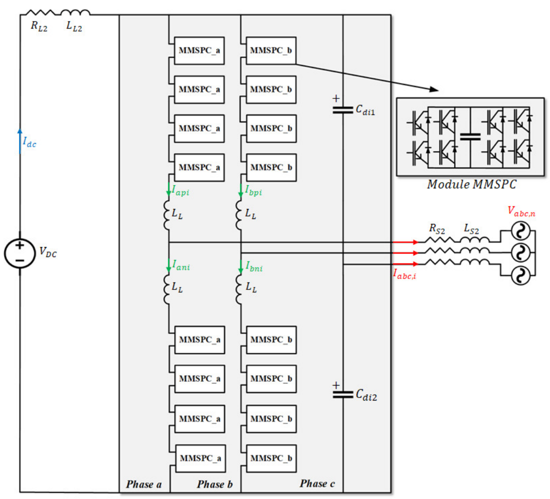

Figure 3: Two phase inverter topology

of the positive and negative arms of each phase of the system, while the AC system is interconnected at the midpoints of each phase. In both converters, the AC system is composed by the grid plus a resistance-inductance filter.

The idea of implementing both systems as two-phase converters, is to reduce the number of modules of the converter compared with a traditional MMC 3-phase converter. Indeed, only two phases of the converter are needed to be able to control the 3-phase currents coming from the electrical grid. In this way, a significant cost reduction of the system is achieved since fewer modules and communication systems are required for the total system to operate.

III. Control and Modulation Strategy

The main objective of this work is to develop a simple control method for the proposed system. This is done to avoid the implementation of dedicated control loops for internal balancing of the capacitor voltages of the MMSPC modules and others to reduce circulating current. Therefore, a control scheme for the two-phase rectifier is developed as shown in

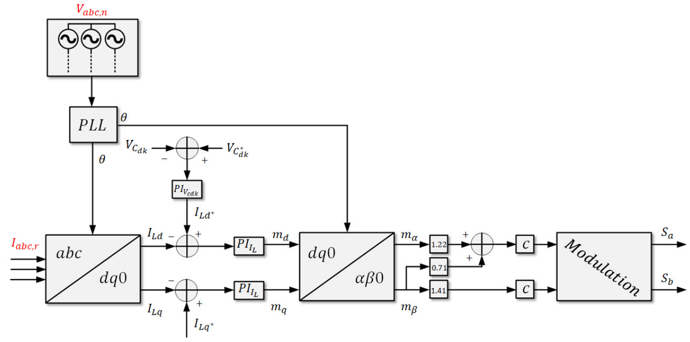

Figure 4: Two phase rectifier topology

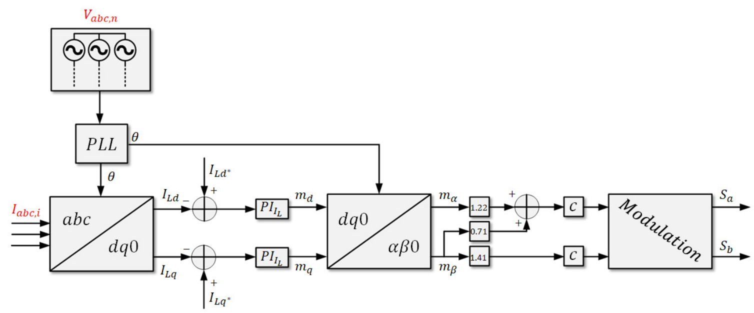

Figure 5: Control inverter topology

Fig. 4 and a control scheme for the two-phase inverter as shown in Fig. 5.

The objective of the rectifier control loop is to keep the voltage in the DC-Link balanced through the implementation of a cascade loop where the voltage in the capacitor C_{dk} is controlled by the current of the AC system 1 connected to the rectifier. On the other hand, the objective of the inverter control loop is to control the AC current injected to the AC system 2.

To control the DC and AC current component of the rectifier (REC) and inverter (INV) converter, the system model that is used is based on [6]:

$$\left(L_L + \frac{2}{3}L_L\right)\frac{d}{dt}\mathbf{i}_{\mathbf{s}_{\mathbf{REC/INV}}} + \left(R_{L_{REC/INV}} + \frac{2}{3}R_L\right)\mathbf{i}_{\mathbf{s}_{\mathbf{REC/INV}}} = V_{Cdk} - \mathbf{P}(\mathbf{V}_{\mathbf{p}_{\mathbf{REC/INV}}} - \mathbf{V}_{\mathbf{n}_{\mathbf{REC/INV}}}) \tag{1}$$

$$(L_{s_{REC/INV}} + L_L)\frac{d}{dt}\mathbf{i}_{\mathbf{o}_{\mathbf{REC/INV}}} + (R_{s_{REC/INV}} + R_L)\,\mathbf{i}_{\mathbf{o}_{\mathbf{REC/INV}}} = \mathbf{Q}(\mathbf{V}_{\mathbf{p}_{\mathbf{REC/INV}}} - \mathbf{V}_{\mathbf{n}_{\mathbf{REC/INV}}}) \tag{2}$$

Where the DC current of the rectifier and the inverter are equal to the vector $\mathbf{i}_{\mathbf{s}_{\mathbf{REC/INV}}}$, the AC current of both converter is equal to $\mathbf{i}_{\mathbf{o}_{\mathbf{REC/INV}}}$. Moreover, the positive and negative voltage of each phase of the converter and the inverter are $\mathbf{V}_{\mathbf{p}_{\mathbf{REC/INV}}}$ and $\mathbf{V}_{\mathbf{n}_{\mathbf{REC/INV}}}$, respectively. Finally $\mathbf{P}$ and $\mathbf{Q}$ are constant matrices defined in [6].

Each voltage arm of the converter is defined by: $\mathbf{V_{pn_{REC/INV}}} = (m_{DC} \pm m_{AC})\, N v_{dc}$, where v_{dc} is the capacitor voltage reference for each module. It is important to note that since the use of MMSPC modules is being considered, decoupled control of the circulating current component is not necessary. Using (1) and (2) it is possible to tune the PI controllers presented in Figs. 4 and 5.

In [14] the AC modulation indices necessary to operate in a 2-phase system, such as the one proposed in this paper, are defined by:

$$V_{ao} = \sqrt{\frac{3}{2}} V_\alpha^* + \sqrt{\frac{1}{2}} V_\beta^* \tag{3}$$

$$V_{bo} = \sqrt{2} V_\beta^* \tag{4}$$

And in order to keep the phase C capacitors connected to the DC-link voltage balanced in both systems, a correction of factors defined by [14] is implemented:

$$V_\alpha^* = \frac{V_{Cdk}}{V_{Cdk}^*}\left(V_\alpha - \frac{\Delta V}{\sqrt{6}}\right) \tag{5}$$

$$V_\beta^* = \frac{V_{Cdk}}{V_{Cdk}^*}\left(V_\beta - \frac{\Delta V}{\sqrt{2}}\right) \tag{6}$$

Where V_{Cdk} and V_{Cdk}^* are the measured and the reference of the DC transmission system, respectively. ΔV is the difference of the capacitor voltages that are connected in the phase C of each system. These adjustments to the references are shown in detail in the implemented control schemes shown in Fig. 4 and Fig. 5.

To achieve the internal voltage balance between the N modules that are connected in series within an arm of the converter, MMSPC-type modules will be used. These modules allow access to both sides of the capacitor to achieve a parallel interconnection between neighboring cells for certain switching states. Also, the remaining switching states permit to connect the neighboring module in either series, anti-series or bypass.

If the MMSPC modules of the same phase are connected in series (anti-series), the phase output voltage will increase (decrease) in one level. However, if the modules are connected in parallel, the phase output voltage is maintained at the same level, but the parallel connection of two adjacent MMSPC modules generates charge-balancing currents, which allows restoring the voltage balance between the MMSPC modules without the implementation of control algorithms or extra voltage/current sensors [15].

However, to achieve this operation, the modulation strategy of each phase must ensure that the parallel state is implemented the maximum number of times that are possible, and the interval between leveling by parallelization should be kept short, so that it reduces the balancing losses [12]. In specific, the phase-shift pulse width modulation (PS-PWM) framework is implemented in this work [15].

In this way, the system is balanced internally without the need for additional control loops or sensors. In the next section, the effects of applying the control loops in the converter of Fig. 1 are shown.

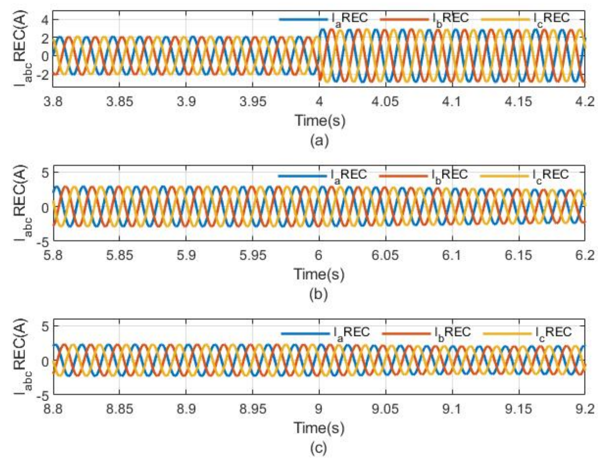

Figure 6: Rectified line current

IV. Simulation Results

The parameters of the simulation are indicated in Table I. The simulation of the two-phase converter is developed for a time of $0 < t < 14$ s. The response of the control loops is validated by making changes to the internal references of these such that in $t = 4$ s the i_q component of the rectifier loop changes from 0 A to 2 A and in $t = 6$ s changes from 2 A to -2 A. In $t = 6$ s the i_d component of the inverter loop changes from 2 A to 1 A and in $t = 9$ s changes from 1 A to -1 A.

A. *Rectified and inverter line currents*

The behavior of line currents for the rectifier and inverter are studied. In Fig. 6, changes in the rectifier line current amplitude are observed, such as 2 A at $t = 3.8$ s and 3 A at $t = 4.1$ s due to changes implemented in the rectifier control loop. From Fig. 7 it is observed that the inverter requests a

Table I: Simulation Parameters

Parameter	Value
DC voltage system V_{DC}	400 V
Carrier frequency of modulation framework	4.5 kHz
Arm Inductance L_L	5 mH
AC output frequency	50 Hz
AC peak voltage $V_{abc,n}$	100 V
DC module voltage v_{dc}	100 V
Capacitance C_{dk}	2200 μF
Capacitance C_{dr1},C_{dr2},C_{di1},C_{di2}	4400 μF
Inductance L_{S1},L_{S2},L_{L1},L_{L2}	10 mH
Filter resistance R_{S1},R_{S2}	0.1 Ω
Filter resistance R_{L1},R_{L2}	0.5 Ω

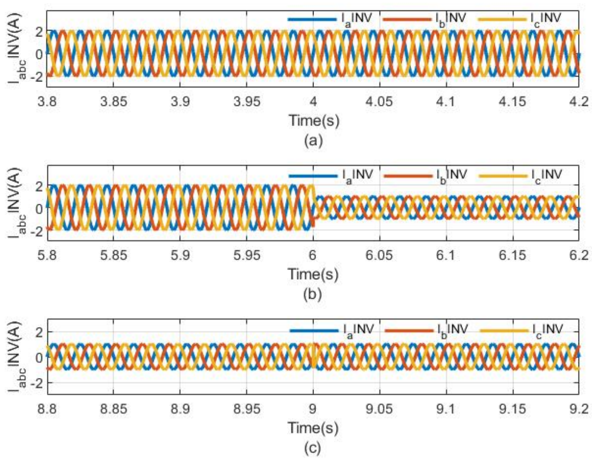

Figure 7: Inverter line current

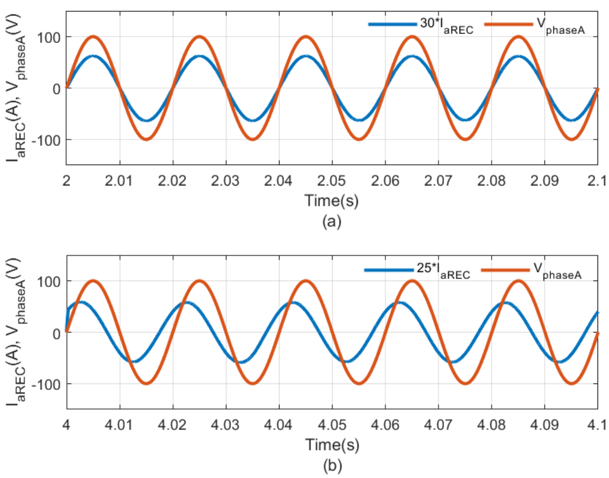

Figure 8: Comparison of phase voltages with phase currents

current of 2 A by design and in $t = 6$ s its amplitude is modified according to the set point change forced. A balanced operation and a high quality power factor are observed for both the rectifier and for the inverter currents, due to the multilevel voltage waveform enabled by the proposed system. Fig. 8 shows the effect of the change in the i_q component of the rectifier control loop, in particular, at $t = 4$ s a phase shift is observed between the voltage and the line current such that the current leads the voltage.

B. Inverter and rectifier arm voltages

The behavior of the arm voltages of the converter in Fig. 1 is discussed in this section. From Fig. 9 it can be observed that the arm voltage of the two-phase rectifier is multilevel for phases A and B, this being a characteristic of MMC, but phase C has a constant value in steady state that corresponds to half the voltage of DC-Link. . The same idea applies to

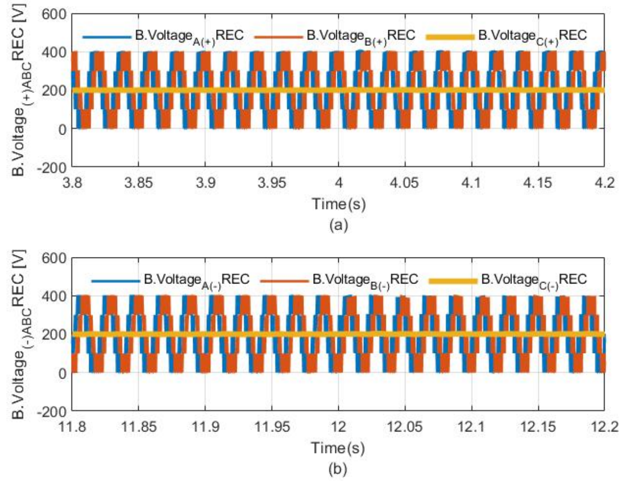

Figure 9: Rectifier arm voltages

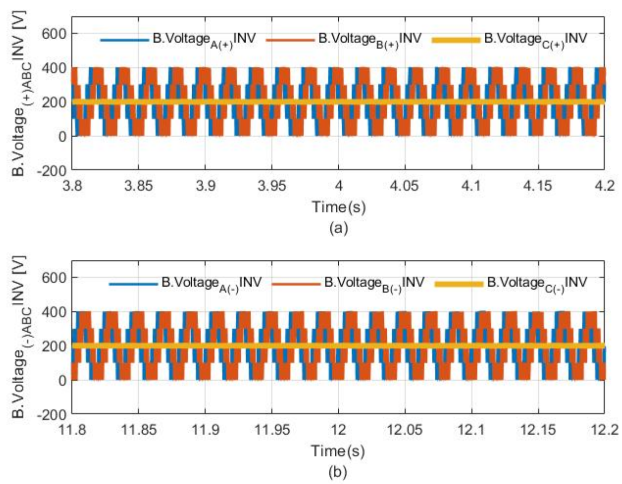

Figure 10: Inverter arm voltages

the two-phase inverter whose arm voltages are observed in Fig. 10.

C. Modules capacitor voltages

The use of MMSPC modules allows the voltage balance of the converter capacitors for phase A (positive and negative arm) and phase B (positive and negative arm) as illustrated in Fig. 11 and Fig. 12. It is observed that the voltage of the capacitor of each module is balanced around 100 V, regardless of the changes that occur in the internal references of the control loops. It can be seen that internal voltage balance is achieved without dedicated control stages or additional sensors. So, since the converter has $N = 4$ cells per arm, the 400V voltage at the DC port is shared equally between them.

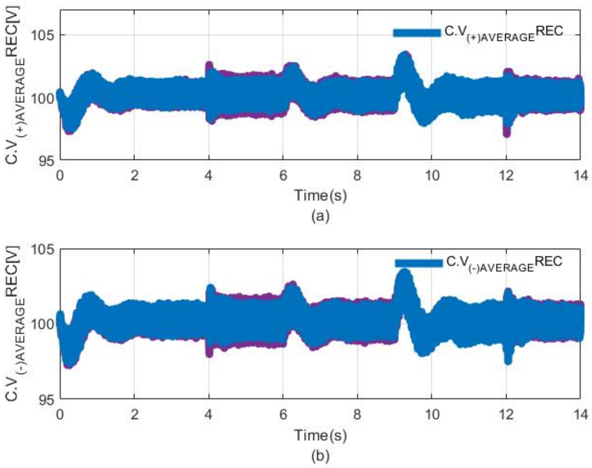

Figure 11: Capacitor voltage average rectified

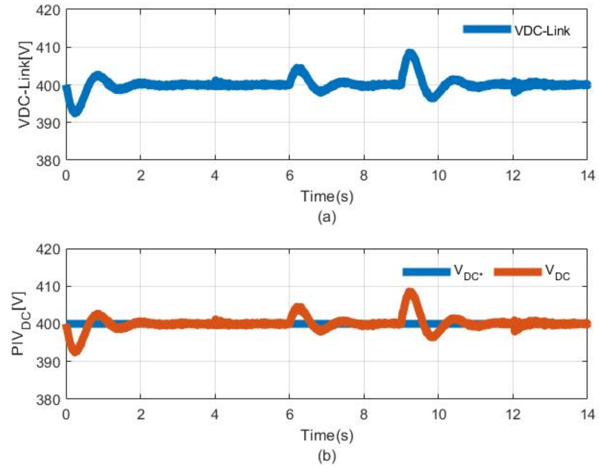

Figure 13: VDC-Link and PIV_{DC}

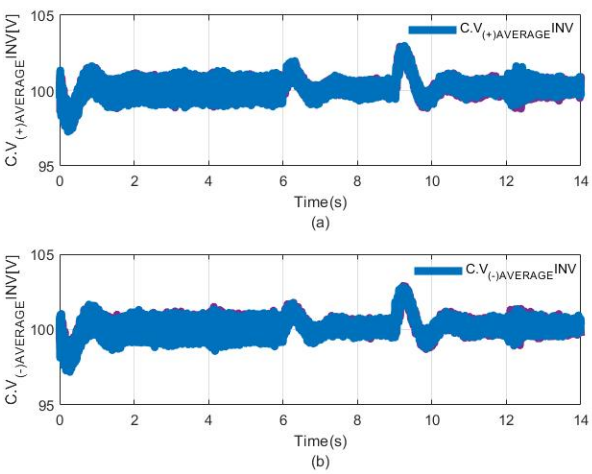

Figure 12: Capacitor voltage average inverter

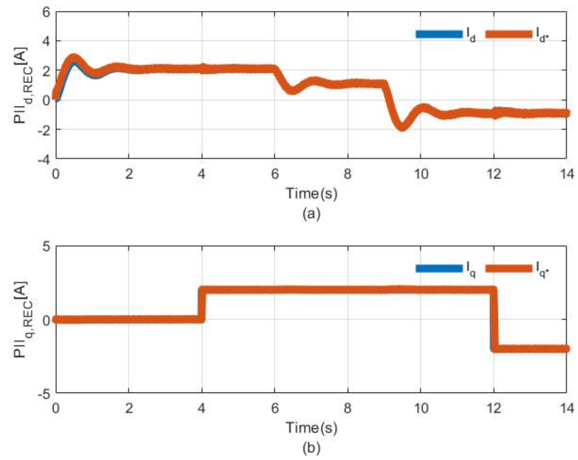

Figure 14: PI control rectifier

D. Control loop response

Fig. 13 presents the voltage in the DC-Link in a) and the PIV_{DC} in the cascade loop of the rectifier in b). It is possible to appreciate that the voltage of the transmission system follows its reference without difficulties.

E. Modulation index

Fig. 16 and Fig. 17 shows the modulation index m_α and m_β that is obtained from the control loop implemented for the two-phase rectifier and two-phase inverter. These modulation index, which corresponds to the AC modulation index of the MMC, vary in a range of $-0.5 \leq m_\alpha \leq 0.5$ and $-0.5 \leq m_\beta$ ≤ 0.5 being these desired values since the modulation index of a MMC under the proposed control premises is the sum of $m_{DC} = 0.5$ and m_{AC}.

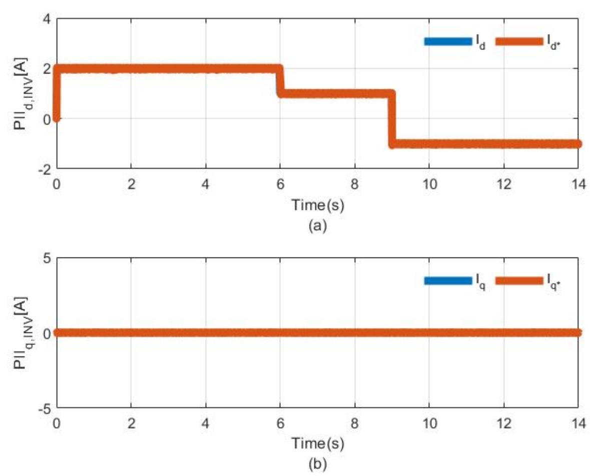

Figure 15: PI control inverter

V. Conclusions

In this paper, a two-phase MMC system based on MMSPC modules for HVDC applications is presented. The results

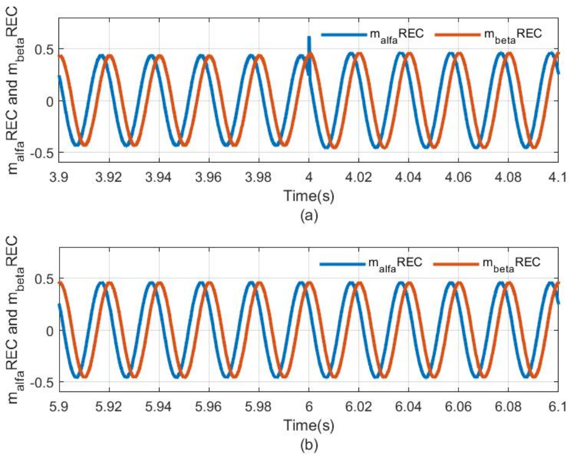

Figure 16: Modulation indices m_α and m_β two-phase rectifier control loop

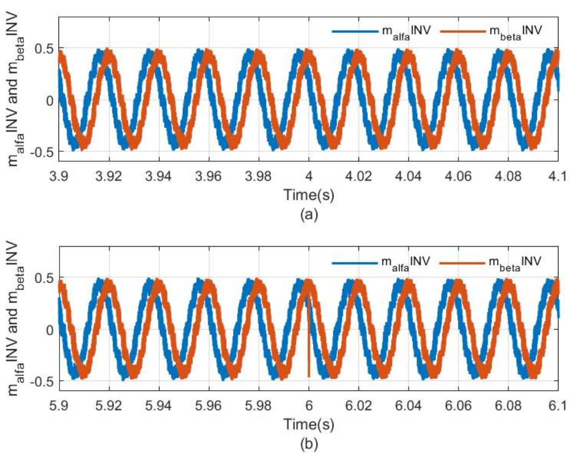

Figure 17: Modulation indices m_α and m_β two-phase inverter control loop

obtained show that with a two-phase MMC system it is possible to optimally control a 3-phase currents of the electrical grid, together with maintaining the internal voltage balance of all the capacitors of the MMC modules. The objective to implement HVDC systems based on two-phase MMC and based on MMSPC cells, is to demonstrated that is possible to reduce costs of the total system, associated with the operation with one less phase in each MMC converter, together with the ability to not require monitoring systems or control loops for maintain the internal voltage balance of each module, thanks to the MMSPC cells.

VI. Acknowledgment

This work was supported by the following projects from the Agencia Nacional de Investigación y Desarrollo (ANID): FONDECYT-R Grant No. 1230306, REDES-PCI 190108, AC3E (ANID/Basal/FB0008), Fondo de Actividades Académicas FAA-UCSC, Centro de Energía UCSC and SERC Chile (ANID/FONDAP/1522A0006). Abraham M. Alcaide gratefully acknowledges to the Contratación de Personal Investigador Doctor. (Convocatoria 2019) 43 Contratos Capital Humano Línea 2. Paidi 2020, supported by the European Social Fund and Junta de Andalucía. and the Spanish Ministry of Universities under the grant Jose Castillejo 2023, CAS22/00425.

References

[1] A. Dekka, B. Wu, R. L. Fuentes, M. Perez, and N. R. Zargari, "Evolution of Topologies, Modeling, Control Schemes, and Applications of Modular Multilevel Converters," *IEEE Trans. Emerg. Sel. Topics Power Electron.*, vol. 5, no. 4, pp. 1631–1656, Dec 2017.

[2] M. A. Perez, S. Bernet, J. Rodriguez, S. Kouro, and R. Lizana, "Circuit Topologies, Modeling, Control Schemes, and Applications of Modular Multilevel Converters," *IEEE Trans. Power Electron.*, vol. 30, no. 1, pp. 4–17, Jan 2015.

[3] J. Rodriguez, S. Bernet, B. Wu, J. O. Pontt, and S. Kouro, "Multilevel Voltage-Source-Converter Topologies for Industrial Medium-Voltage Drives," *IEEE Trans. Ind. Electron.*, vol. 54, no. 6, pp. 2930–2945, Dec 2007.

[4] S. Kouro, M. Malinowski, K. Gopakumar, J. Pou, L. G. Franquelo, B. Wu, J. Rodriguez, M. A. Perez, and J. I. Leon, "Recent Advances and Industrial Applications of Multilevel Converters," *IEEE Trans. Ind. Electron.*, vol. 57, no. 8, pp. 2553–2580, Aug 2010.

[5] L. G. Franquelo, J. Rodriguez, J. I. Leon, S. Kouro, R. Portillo, and M. A. M. Prats, "The Age of Multilevel Converters Arrives," *IEEE Ind. Electron. Mag.*, vol. 2, no. 2, pp. 28–39, June 2008.

[6] R. Lizana, M. A. Perez, D. Arancibia, J. R. Espinoza, and J. Rodriguez, "Decoupled Current Model and Control of Modular Multilevel Converters," *IEEE Trans. Ind. Electron.*, vol. 62, no. 9, pp. 5382–5392, Sept 2015.

[7] F. Helling, S. Götz, A. Singer, and T. Weyh, "Fast modular multilevel series/parallel converter for direct-drive gas turbines," in *2015 IEEE NW Russia Young Researchers in Electrical and Electronic Engineering Conference (EIConRusNW)*, Feb 2015, pp. 198–202.

[8] C. Wang, Z. Li, D. L. K. Murphy, Z. Li, A. V. Peterchev, and S. M. Goetz, "Photovoltaic Multilevel Inverter with Distributed Maximum Power Point Tracking and Dynamic Circuit Reconfiguration," in *2017 IEEE 3rd International Future Energy Electronics Conference and ECCE Asia (IFEEC 2017 - ECCE Asia)*, June 2017, pp. 1520–1525.

[9] S. M. Goetz, Z. Li, X. Liang, C. Zhang, S. M. Lukic, and A. V. Peterchev, "Control of Modular Multilevel Converter With Parallel Connectivity - Application to Battery Systems," *IEEE Trans. Power Electron.*, vol. 32, no. 11, pp. 8381–8392, Nov 2017.

[10] R. L. F., S. Rivera, Z. Li, J. Luo, A. V. Peterchev, and S. M. Goetz, "Modular multilevel series/parallel converter with switched-inductor energy transfer between modules," *IEEE Transactions on Power Electronics*, vol. 34, no. 5, pp. 4844–4852, 2019.

[11] S. M. Goetz, A. V. Peterchev, and T. Weyh, "Modular Multilevel Converter With Series and Parallel Module Connectivity: Topology and Control," *IEEE Trans. Power Electron.*, vol. 30, no. 1, pp. 203–215, Jan 2015.

[12] H. Bahamonde I., S. Rivera, Z. Li, S. Goetz, A. Peterchev, and R. Lizana F., "Different parallel connections generated by the modular multilevel series/parallel converter: an overview," in *IECON 2019 - 45th Annual Conference of the IEEE Industrial Electronics Society*, vol. 1, 2019, pp. 6114–6119.

[13] R. Lizana, S. Rivera, F. Figueroa, F. Flores-Bahamonde, J. Rodriguez, and S. M. Goetz, "Hybrid energy storage system based on a multioutput multilevel converter," *IEEE Journal of Emerging and Selected Topics in Power Electronics*, vol. 11, no. 4, pp. 3864–3873, 2023.

[14] M. B. de Rossiter Correa, C. B. Jacobina, E. R. C. da Silva, and A. M. N. Lima, "A general pwm strategy for four-switch three-phase inverters," *IEEE Transactions on Power Electronics*, vol. 21, no. 6, pp. 1618–1627, 2006.

[15] M. Correa, S. Rivera, and R. L. F, "Hybrid energy storage system based on modular multilevel series parallel converter," in *IECON 2022 – 48th Annual Conference of the IEEE Industrial Electronics Society*, 2022, pp. 1–5.